



Development of the Nanoemulsion Formulation Containing Ylang Ylang Essential Oil for Topical Applications, and Evaluation of Its *In Vitro* Cytotoxicity as well as ADMET Profile

Nesrin Karabatak^{1†}, Bahar Gok^{2†}, Yasemin Budama Kilinc^{2,3*}

¹Graduate School of Natural and Applied Science, Yildiz Technical University, 34220 Istanbul, Turkey.

²Faculty of Chemical and Metallurgical Engineering, Department of Bioengineering, Yildiz Technical University, 34220 Istanbul, Turkey.

³Health Biotechnology Joint Research and Application Center of Excellence, 34220 Istanbul, Turkey.

[†]The authors contributed equally.

Abstract: Ultraviolet (UV) rays damage DNA, causing adverse effects such as photoaging and cancer on the skin. For the well-being of individuals, there is a need to develop innovative skin products with high effectiveness using protective and therapeutic agents. In our study, a nanoemulsion (NE) formulation containing Ylang-ylang essential oil (YO), which has many biological active properties such as antimicrobial, antioxidant, anti-inflammatory, and anticancer, was produced by the ultrasonic emulsification method and characterized. The thermodynamic stability was evaluated, and its release profile determined the dialysis membrane technique. The cytotoxic effect of YO-NE was examined with the *in vitro* method on the HacaT cell line using the MTT method and *in silico* method using the ADMET profile. Dynamic light scattering (DLS) results showed that the average droplet size of the YO-NE formulation was 184.1 ± 2.307 nm, the polydispersity index (PdI) was 0.151 ± 0.006 , and the Zeta potential (ζ) -10.8 ± 0.400 mV. As a result of release studies, it was observed that $99.98 \pm 1.00\%$ of YO release from NE occurred within 5 hours. Based on the thermodynamic stability test results, it was determined that the developed formulation did not show sedimentation or phase separation. Cytotoxicity results revealed that the YO-NE formulation was safe. All the results indicated that the YO-NE formulation might be considered a non-toxic product candidate with physicochemical properties suitable for topical use.

Keywords: Nanoemulsion (NE), Ylang-ylang essential oil (YO), Cytotoxicity, Topical application.

Submitted: January 13, 2024. **Accepted:** June 23, 2024.

Cite this: Karabatak N, Gok B, Budama Kilinc Y. Development of the Nanoemulsion Formulation Containing Ylang Ylang Essential Oil for Topical Applications, and Evaluation of Its *In Vitro* Cytotoxicity as well as ADMET Profile. JOTCSA. 2024;11(3): 1181-96.

DOI: <https://doi.org/10.18596/jotcsa.1418645>

***Corresponding author's E-mail:** yaseminbudama@gmail.com

1. INTRODUCTION

Skin, the largest body organ, plays a critical role in maintaining homeostasis and creates a protective barrier between the environment and the body (1). However, exposure of this barrier to excessive sunlight may disrupt the barrier function of the skin (2). Exposure to ultraviolet (UV) radiation can lead to the overproduction of reactive oxygen species (ROS) in skin cells, DNA damage, lipid peroxidation, protein modification, and cell apoptosis (3). These factors can lead to skin problems such as photoaging, wrinkles, inflammation, and even skin cancer (4). Plants or bioactive components obtained from plants can be used to overcome these problems (5-7).

Plants and active substances derived from plants are widely used in producing cosmetic materials for protection from UV rays, antioxidants, cell renewal and minimizing the effects of photoaging (8). Essential oils (EOs) from plants, their usage in the plant defence mechanisms against different parasite species and infections is used in various medical approaches with biochemical effects such as antiviral, anticancer, antibacterial, and anti-inflammatory activities (9). Ylang-ylang, also commonly known as *Cananga odorata*, is a fast-growing tree commonly found in tropical Asian countries such as Malaysia, Philippines, Indonesia and some islands of the Indian Ocean. Ylang-ylang EOs are currently widely used in the food, perfume,

cosmetics industry and aromatherapy to treat many diseases such as asthma, fever, inflammation, wounds, microbial infections, colds, etc (10,11). The Ylang-ylang plant and especially the EOs obtained from it contain antioxidant components. The antioxidant effects of EO obtained from ylang-ylang help to reduce oxidative stress and positively support body health by fighting free radicals that cause cellular damage (12).

Although EOs have many biological activities, their clinical applications are limited due to their hydrophobic structure and poor stability in different environmental conditions such as air, light, humidity, and high temperature. To overcome the limitations in the clinical use of EOs, they are prepared in nano-sized and suitable dosage forms for the application method (13). The development of innovative formulations in the field of nanomedicine has enabled increasing the therapeutic efficacy and reducing the toxicity of natural compounds and their bioactive components (14-16).

Among nanoformulations as nanoemulsions (NEs), frequently preferred for topical use, are translucent and/or transparent emulsions characterized by nano-sized droplets (17). When used as a topical carrier, small droplets have a large surface-to-volume ratio, allowing the activated compound to spread easily into the skin and provide high absorption. In addition, nanoemulsions can increase the solubility of lipophilic compounds and change the skin's diffusion barrier depending on the nanoemulsion's composition. Thus, they may enable the drug to penetrate better into the skin layers (18,19). The nanometer size of NE improves its transmission target and specificity, making it more perfect and effective than pure EO (20). NE formulations are safe for human health. They increase the solubility, bioabsorption, biomembrane permeability, and bioavailability of poorly soluble active substances. Additionally, NEs are biocompatible, biodegradable, and do not have mutagenic effects. Thanks to their controlled release properties, NEs minimize the toxicity of the active ingredient and contribute to a better therapeutic effect (21,22). Additionally, NEs contain fewer surfactants than microemulsions, and these surfactants are environmentally friendly, cost-effective, and economically viable (20).

In this study, YO-NE nanoformulation was prepared using the ultrasonic emulsification method and then characterized by different techniques. DLS was used to determine parameters such as average droplet size, ζ potential, and PdI. The thermodynamic (centrifugation and thermal stress test) and physicochemical stability of the YO-NE formulation were evaluated. The release profile of the YO-NE formulation was determined with a UV-Vis spectrophotometer using the dialysis membrane method. The cytotoxic activity of YO-NE was evaluated by the MTT method using the HacaT cell line. Finally, the ADMET profile of YO was considered.

2. EXPERIMENTAL SECTION

2.1. Material

Ylang-ylang oil was purchased from Aksuvital, Ethanol, Kolliphore® P-188, DL-alpha tocopherol acetate from Sigma-Aldrich; undecyl alcohol and isodecyl neopentanoate were purchased from Schülke. Caprylic/capric triglyceride was purchased from Gattefosse. The HaCaT cell line used in the MTT assay was purchased from Thermo Fisher Scientific, MTT from Biomaterials, and trypsin/EDTA (0.25%) was purchased from Gibco. Fetal Bovine Serum (FBS) and penicillin-streptomycin Solution were purchased from Biological Industries.

2.2. Method

2.2.1. Development of the YO-NE

YO-NE formulation, in which the aqueous phase is a continuous phase (O/W), was prepared using the ultrasonic emulsification method (23). The water phase of NE was obtained by dissolving 7.5% Kolliphore® P-188 in water. The oil phase was formed by the addition of 1% undecyl alcohol, 1.25% transcutool, 1.5% isodecyl neopentanoate, 10% caprylic capric triglyceride, 0.2% DL-alpha tocopherol acetate, 3% Labrafil and 0.5% YO. These phases were prepared separately, and then the water phase was added to the oil phase. The premixing step was performed using a homogenizer (Witeg, Germany) at 8100 rpm for 5 minutes. After pre-mixing, the emulsion was ultrasonicated at 50% amplitude for 20 minutes using a 20 kHz and 750 W sonicator (Ultrasonics, USA).

2.2.2. Analysis of droplet size, PdI and ζ potential of YO-NE

The parameters such as PdI, average droplet size, and Zeta potential (ζ) values of YO-NE were measured using Zeta Sizer Nano ZS (Malvern Instruments, UK). All measurements were performed at 25°C. Specimens were diluted as 1:100 in sterile water and carried out in triplicate (24).

2.2.3. Analysis of pH and electrical conductivity of YO-NE

A pH meter (Ohaus® STARTER 3100M) with a conductivity probe was used to determine the electrical conductivity and pH of the YO-NE formulation. All analyses were performed in triplicate at 25°C.

2.2.4. Active ingredient content analysis

Active ingredient content analysis is used to assess the stability of drugs in pharmaceutical formulation. In this experiment, the YO-NE formulation (250 μ L) was dissolved in 10 mL ethanol and sonicated in an ultrasonic bath for 30 min (25). The YO content in the sample was then determined using the equation for the spectrophotometric analysis curve of YO.

2.2.5. Morphology analysis

The morphology of YO-NEs was examined by transmission electron microscopy (TEM) (JEOL TEM 1400 Plus). A carbon-coated grid was used in the analyses. A sufficient amount of the formulation was placed on the grid, and images were displayed under a voltage of 80 kV (26).

2.2.6. YO-NE accelerated stability tests

Following the preparation of the YO-NE formulation accelerated thermodynamic stability tests consisting of centrifugation and thermal stress tests were carried out within 24 hours. 0.5 g of the YO-NE formulation was centrifuged at 4500 rpm for 30 minutes at $25 \pm 1^\circ\text{C}$. Macroscopically, it was evaluated for any phase separation or turbidity (27). For thermal stability testing, 0.5 g of YO-NE formulation was carried out in a water bath at $40\text{--}80^\circ\text{C}$ with temperature increments of 5°C each. The thermal stability test of the YO-NE formulation was evaluated in terms of organoleptic features organoleptic aspects such as color, odor, texture and phase separation.

2.2.7. Calibration curve

Seven different YO concentrations (2.34, 4.68, 9.36, 18.75, 37.5, 75 and 150 $\mu\text{g}/\text{mL}$) were prepared in ethanol. Then, the absorbance values of these samples were measured with a UV-Vis Spectrophotometer (Shimadzu, Japan) at 283.2 nm, and the calibration curve was drawn (28). This curve was used to determine the amount of YO in the release study of YO-NEs.

2.2.8. Release study

Since the YO-NE formulation is intended for topical application, the release study was performed at skin pH 5.5 and temperature (32°C) (29,30). 1 g of YO-NE was added to the dialysis capsule, and 1 mL of release medium was taken at specified time intervals from a water bath shaking at 120 rpm and added with an equal volume of fresh release medium. The amount of YO released was determined by analyzing the absorbance of the samples with a UV-Vis spectrometer at 283.2 nm. YO release (%) was calculated using Equation (1).

$$\text{Release\%} = \frac{\text{Released YO}}{\text{Total YO}} \cdot 100 \quad (1)$$

2.2.9. Preparation of cell culture

The cytotoxic effect of YO and YO-NE on HaCaT cells was evaluated using MTT assay. HaCaT cell line was incubated in Dulbecco's Modified Eagle's Medium (DMEM) medium containing 100 U/mL penicillin-100 g/mL streptomycin antibiotic and 10% Fetal Bovine Serum (FBS) in a 5% CO_2 incubator at 37°C until 80% confluent. The proliferating cells were washed with 5 mL sterile phosphate buffer solution (PBS). To lift off the cells from the flask, 1 mL of trypsin-EDTA was added and incubated for 5 minutes. To neutralize the effect of trypsin, 5 mL of culture medium was added to the cells and the cells were centrifuged at 123 g for 5 minutes. The supernatant was discarded, and the pellet was dissolved in 1 mL of medium and counted on a thoma slide (31).

2.2.10. Cell viability test (MTT)

The *in vitro* safety of YO and YO-NE was evaluated by MTT test using the HaCaT cell line. In this method, cells were seeded in a 96-well plate ($1 \times 10^4/\text{well}$) and incubated for 24 hours at 37°C in a humidified incubator with 5% CO_2 . After incubation, five different concentrations of YO and YO-NE (0.25, 0.5, 1, 3 and 5 mg/mL) were added to the wells and

incubated for 24 hours. In this test system, 0.1% DMSO was used to prepare concentrations of YO. DMEM was used to prepare the concentrations of NEs. For YO, DMEM containing 0.1% DMSO was used as a control, while for YO-NE, only DMEM was used. Ten μL of MTT solution was added to each well and incubated for 4 hours. The medium was carefully removed, and the colored formazan crystals were dissolved in 100 μL of dimethyl sulfoxide (DMSO). The absorbance given by the cells in the plates was measured at 570 nm using a microplate reader. YO and YO-NE untreated control value was expressed as 100% cell viability. Equation (2) was used to determine cell viability.

$$\text{Cell viability} = \left(\frac{\text{OD}_{570} \text{ of sample}}{\text{OD}_{570} \text{ of control}} \right) \times 100 \quad (2)$$

2.2.11. Physicochemical and pharmacokinetic analyses of linalool and germacrene-D

Linalool is found in many aromatic plant families, such as Rutaceae and Lamiaceae. Linalool is a naturally occurring acyclic monoterpene alcohol. Numerous traditional and edible plants, including coriander, peppermint and cinnamon, produce essential oils containing linalool (32). The Food and Drug Administration (FDA) has deemed linalool as GRAS safe (GRAS) as a synthetic flavoring agent as well as an excipient in foods for humans (21 CFR 182.60) and as an ingredient in animal drugs and foods (21 CFR 582.60) (33). The chiral hydrocarbon germacrene-D is a widely available plant component that is recognized as a critical intermediate in the biosynthesis of many sesquiterpenes (34). These sesquiterpene hydrocarbons are biosynthetic precursors of various (often oxidized) structures from which humans have exploited many compounds with significant medicinal and other bioactivities (35).

Kalagatur et al. (2018) (11) characterised ylang-ylang oil by GC-MS and reported that the main compounds in the oil were linalool (29.15%), germacrene-D (11.82%) and thymol (8.45%). In this study, physicochemical and pharmacokinetic analyses were carried out due to the high amounts of linalool and germacrene-D compounds in ylang-ylang oil.

Drug susceptibility characteristics were analyzed using SwissADME (absorption, distribution, metabolism and excretion) and the PkCSM tool to predict crucial pharmacokinetic properties such as drug candidate molecules' absorption, distribution, metabolism, excretion, and toxicity (ADMET). The canonical simplified molecular input line entry system (SMILES) format of the compound was retrieved from PubChem (<https://pubchem.ncbi.nlm.nih.gov/>) and entered into SwissADME and PkCSM (<http://www.swissadme.ch/>) (<https://biosig.lab.uq.edu.au/pkcsm/>) has been sent (36,37). Drug susceptibility is determined by Lipinski's rule of five (RO5) (38).

2.2.12. Estimation of biological activity

The evaluation of the overall biological potential of the compounds was performed using PASS (<http://195.178.207.233/PASS/index.html>). This software estimates the predicted activity spectrum of a compound with probability (P_a = probability of 'activity' and P_i = probability of 'inactivity'). The cut-off value was set as $P_a \geq 0.7$ (39). This method is based on the training set's structural activity relationship (SAR) analysis, which contains more than 205,000 compounds exhibiting more than 3750 biological activities. Compounds that show a probability that the P_a value is higher than the P_i value are those considered to be possible for a specific pharmacological activity (40).

3. RESULTS AND DISCUSSION

3.1. Characterization of YO-NE

The ultrasonic homogenization method is a fast and effective method to create stable NEs with appropriate droplet sizes and low PdI (41,42). In this study, NE formulation was synthesized with ultrasonic homogenization, followed by characterization and stability studies.

DLS, one of the most preferred methods, was employed to determine the hydrodynamic size, PdI, and ζ potential value of the synthesized NE (43,44). The results were given in Figure 1 and Figure 2. The average droplet size of the empty NE was 183.2 ± 1.498 nm. However, the average droplet size of YO-NE was 187 ± 2.307 nm. The most important advantage of NEs over emulsions is that they are nanosystems with small droplet sizes of 20-200 nm (45). The small droplet size of NEs provides many advantages, such as overcoming difficulties, separation, flocculation and coalescence due to gravity (46,47). Many studies have reported that droplet sizes between 100-200 nm may benefit NEs in topical applications due to their excellent penetrability and controlled release capabilities (48,49). Based on the average droplet size data, the

YO-NE formulation was considered suitable for topical administration.

PdI value is essential for the homogeneity of droplet sizes in NE and the stability of the formulation. A PdI value of <0.1 means a narrow size distribution of droplets, and this is the indication of the formulation homogeneity. A PdI value of >0.2 indicates a wide dimensional distribution of droplets, i.e., heterogeneity of the formulation (50). It was determined that the PdI value of empty NE was 0.190 ± 0.020 and the PdI value of YO-NE was 0.151 ± 0.006 . The results showed that the droplets formed have a tight size range, i.e., homogeneous.

Ozdemir et al. (2023) (51) found that the average droplet size of the NE formulation (F2) containing etodolac was 163.5 ± 2.2 , PdI 0.141 ± 0.02 , zeta potential -33.1 ± 1.7 . Gündel et al. (2020) (52) found the average droplet size of NE formulation containing eucalyptus as 68 ± 0.15 , PdI 0.18 ± 0.01 , zeta potential -9.09 ± 0.65 . Our results coincided with those presented in previous studies in the literature.

ζ potential is used to calculate the charge on the surface of NE droplets and to indirectly determine the electric charge of particles in a heterogeneous system (53). The minus charge in the ζ potential value is due to the carboxylic acid groups of fatty acids used in the formulation of fatty acids (54). The ζ potential of empty NE was found to be -10.7 ± 0.252 mV and the ζ potential of YO-NE was found to be -10.8 ± 0.400 mV.

Kildaci et al. (2021) (55) obtained a stable LSO-NE for topical application, an acceptable mean droplet size of 90.61 ± 0.94 , a PdI value of 0.15 ± 0.008 and a zeta potential value of 9.64 ± 0.55 mV. Kilinc et al. (2022) (56) obtained a stable CA-NE for topical application and found an average droplet size of 120.4 ± 6.39 nm, PdI value of 0.180 ± 0.018 , and zeta value of 11.5 ± 1.15 mV. This study's results were similar to those presented in previous studies in the literature.

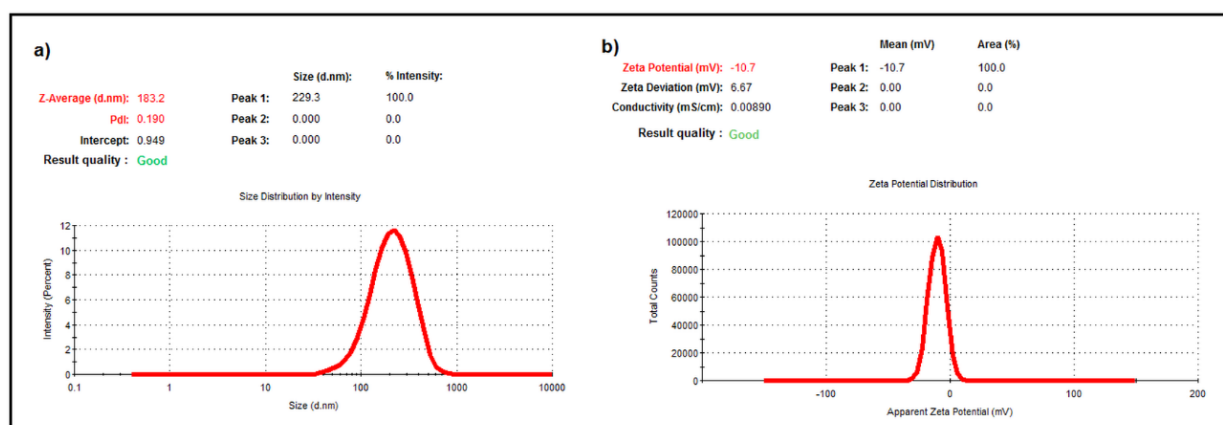


Figure 1: DLS analyses of the empty NE. (a) Average droplet size plot and PdI, (b) ζ potential graph.

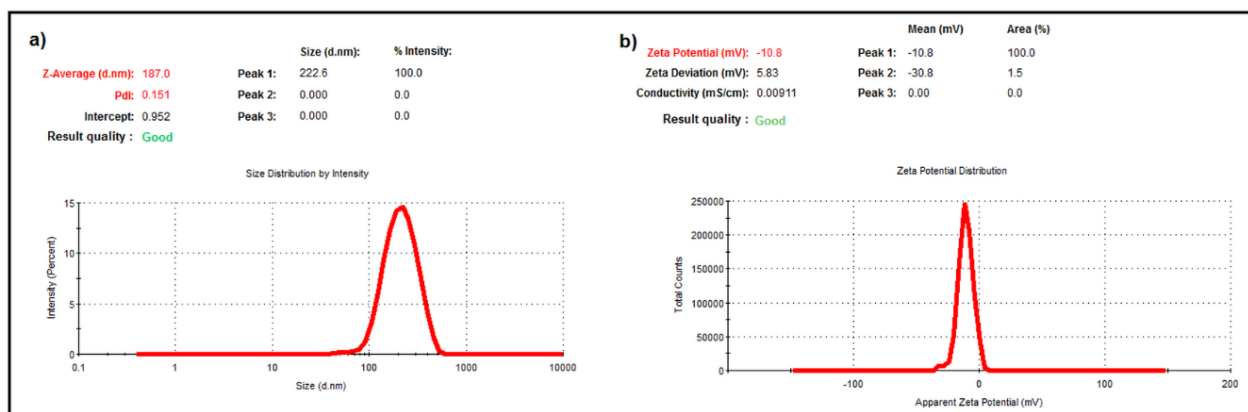


Figure 2: DLS analyses of YO-NE (a) Average droplet size plot and PdI, (b) ζ potential graph.

3.2. pH and Conductivity

The pH value is crucial for assessing the stability of nanoemulsions. pH changes in the formulation suggest the possibility of chemical reactions leading to problems in the stability and quality of the final product (57). The pH value of the skin is approximately 5.5 and generally a pH in the range of 4.0 to 7.0 is appropriate for topical applications. In conclusion, according to the data obtained from our study, the pH value of YO-NE is 5.83, which makes it appropriate for topical application (Table 1). Rashid et al. (2021) (58) determined the pH value of methotrexate-loaded nanoemulsion as 5.81 ± 0.22 , which is an acceptable value for application as transdermal systems since it is within the specified range scale of the physiological pH of the skin. Hammodi et al. (2020) (59) found the pH value (5.96 ± 0.025) of letrozole loaded NE formulation to be in the acceptable range for topical use. Our results are similar to those results presented in previous studies in the literature.

Conductivity is the measurement of the amount of free ions and water present in the solution and the determination of its response. The O/W formulation is suitable for use in the cosmetic industry as its structure is less oily after topical application (60). This parameter allows the determination of the kind of NE prepared. The high conductivity of YO-NE ($92.63 \mu\text{S}/\text{cm}$) indicates that the aqueous phase is a continuous phase and the nanoemulsion formed is an oil-in-water nanoemulsion (O/W). In this study, YO-NE formulations' pH and conductivity values are higher than empty-NE (Table 1). Wang et al., (2020) (61) reported the effect of pH on both the hydrodynamic diameter of droplets and the conductivity of NEs. In this effect, the hydrodynamic diameter of the droplets gradually increases with increasing pH. Regulation of pH changes the ionic strength and, therefore, affects the droplet size of NEs. As the pH value increases, the conductivity of NEs gradually increases, which means that the ionic strength increases simultaneously. These results explain why YO-NEs have higher pH and conductivity values than empty-NEs.

Table 1: The pH and conductivity values of NEs. (Data are presented as mean \pm SD).

Formulation	pH	Conductivity ($\mu\text{S}/\text{cm}$)
Empty-NE	4.48 ± 0.02	87.33 ± 0.65
YO-NE	5.83 ± 0.02	92.63 ± 5.90

3.3. Active Ingredient Content Analysis

Active substance content analysis is critical for any dosage form. The amount of active ingredient in the product should not deviate from the amount specified on the label beyond certain limits during the shelf life of the formulation (62). In this study, NE content (%) was determined as $90.00 \pm 0.01\%$ on the day of production. This result shows that it is able to protect the YO loaded in the final NE formulation against degradation.

3.4. Morphology Analysis

Electron microscopy provides high-resolution images for structural examination of droplets in nanoemulsion formulations. Figure 3 shows the TEM image of the YO-NE formulation. TEM analysis supported characterization studies of the synthesized nanoemulsion formulation. The image showed that the formulation had a spherical morphology and a homogeneous and monodisperse distribution, supporting the PdI results obtained from DLS analyses.

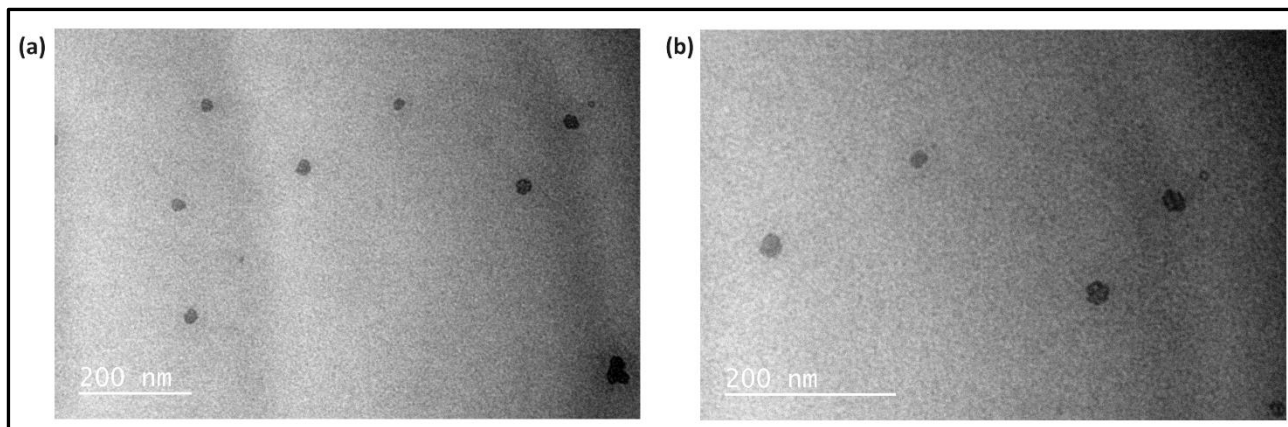


Figure 3: TEM image of YO-NE.

3.5. Accelerated Stability Tests

Stability is essential for formulations developed as product candidates. It provides information about the shelf life of the product candidate. A nanoemulsion formulation must remain physically stable with little or no change in droplet size throughout its shelf life. The creaming and phase separation rate of NEs (regarding shelf life) can be evaluated by gravitational force (63) and thermal stability (64). In the literature, emulsions have been assessed for any phase separation or turbidity as a result of centrifuge testing (27,60,65) and analyzed for organoleptic properties such as colour, odour, texture and phase separation as a result of thermal

stress testing (26,66). YO-NEs showed no physical changes or phase separation following 4,500 rpm gravitational force and thermal stability tests for 30 min (Table 2). In addition DLS results were given in Table 3.

3.6. Calibration Curve of YO

YO solutions were prepared in ethanol at different concentrations (2.34, 4.68, 9.36, 18.75, 37.5, 75 and 150 µg/mL). Then, the absorbance values of these samples were measured at 283.2 nm with a UV-Vis spectrophotometer, and the calibration curve shown in Figure 4 was drawn.

Table 2: Accelerated stability test data of the NEs.

Formulation	Organoleptic properties
Empty NE	Milky aspect
YO-NE	Milky aspect

Table 3: DLS results before and after preliminary stability tests.

Results	Average Droplet Size(nm)	Polydispersity Index (PdI)	Zeta potential (mV)
Before Stability Tests	184.1±2.307	0.151±0.006	-10.8±0.400
After Thermal Test	192.1±5.524	0.143±0.015	-9.31±0.792
After Centrifuge Test	172.5±5.374	0.163±0.042	-11.3±0.070

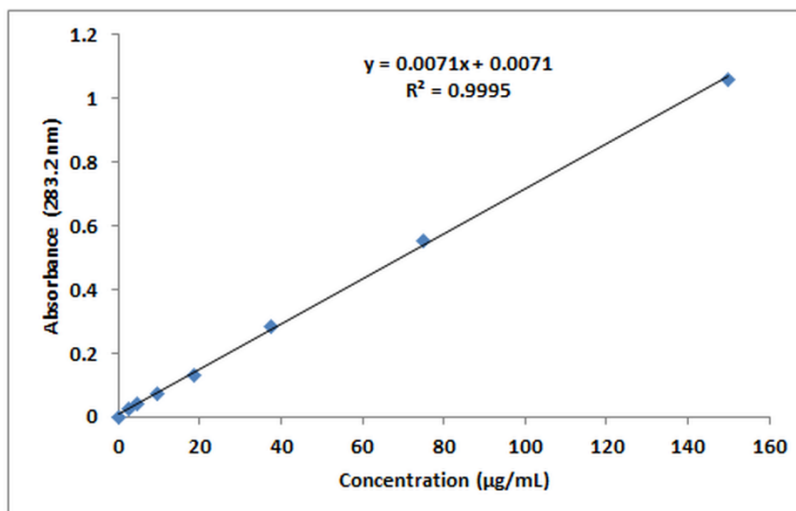


Figure 4: Calibration curve of YO (n=3).

3.7. Release Study Results of YO-NE

Oil-in-water (O/W) type NEs are unique systems that offer higher transparency, stability, biological activity, better physical and chemical properties, and better-controlled release (67). In this study, a release study of YO-NE formulation was carried out by comparing it with YO by diffusion membrane method under simulated skin pH and temperature conditions.

Figure 5 presents the % release of YO as a function of time. As seen in Figure 5, free YO was observed to be released from the membrane very quickly. While 98.84% of YO was released in the first 45 minutes, $99.98 \pm 1.00\%$ of YO was released from YO-NE within 5 hours.

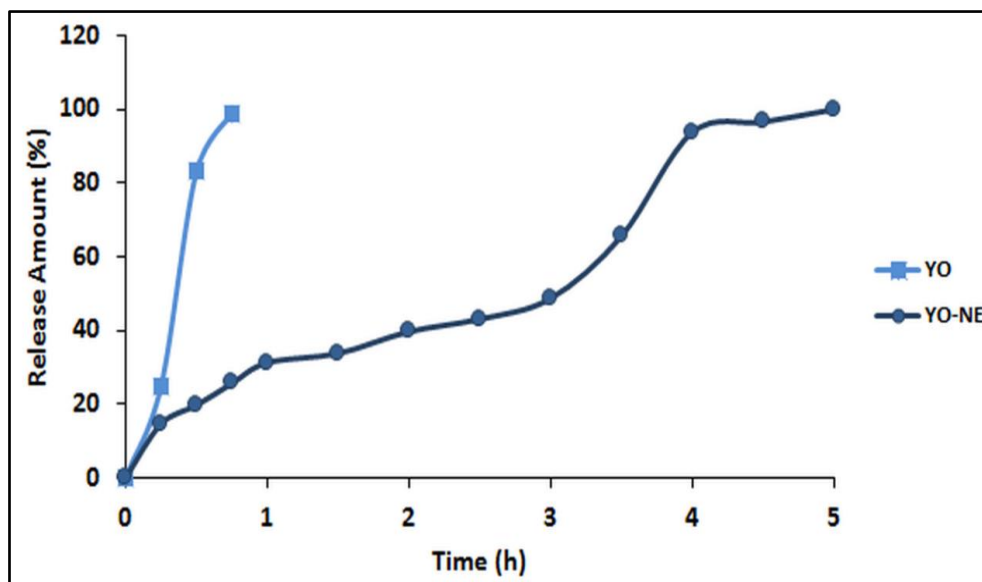


Figure 5: Release profile of YO-NEs.

While free YO molecules are released quickly, the release profile obtained by formulating YO as nanoemulsion ensures continuous release and long-term maintenance of a constant amount of oil (68,69).

The release of active ingredients from the nanoemulsion is controlled by interactions between the drug and surfactant or by partitioning the drug between the oil and water phases. Small droplet size and higher surface area in nanoemulsions will allow adequate release of the loaded drug. The release occurs in a controlled manner (70). Surfactant content is an essential factor affecting the release rate from the oil-containing nanoemulsion system. High surfactant ratio formulations have a slower release rate than low surfactant ratio formulations (71).

Shah et al (2019) (72) developed seven different NE formulations containing moxifloxacin, showing that these formulations released more than 90% of the drug content within 3 hours. Botros et al. (2020) (73) reported that almost all active ingredients were released from the formulation within 4.5 hours. These results are quite suitable for a topical preparation whose skin contact time is generally around 6 hours. Moreover, this short-term release indicates that its active ingredient is suitable for absorption and also provides good bioavailability (73). Our findings are similar to the literature.

3.8. Cytotoxicity Analysis of YO-NE

MTT assay was performed to determine the cytotoxic effect of YO and YO-NE formulation. This assay is

based on the metabolic activity of living cells by reducing MTT to formazan crystals. Since the overall mitochondrial activity of the cell population is related to the number of viable cells, the MTT assay is commonly used to evaluate the cytotoxic effects on cell lines or primary diseased tissues *in vitro* (74,75).

The cytotoxic activity of YO and YO-NE formulation was determined using HaCaT cells. HaCaT cells are easily used in skin toxicity studies due to being the first cell line subjected to cosmetic agents applied to the skin, high experimental reproducibility, ease of use, rapid proliferation and low cost (31). According to ISO standards, cell viability above 80% does not have a cytotoxic effect; 80% to 60% is low; 60% to 40% is medium; and below 40% is cytotoxic (76). The results showed that all concentrations of YO (0.25, 0.5, 1, 3, 5 mg/mL) reduced cell viability in HaCaT cells by $55.75 \pm 3.25\%$, $41.10 \pm 3.64\%$, $40.70 \pm 3.65\%$, $39.66 \pm 4.02\%$, and $31.34 \pm 2.04\%$, respectively ($p < 0.05$). All concentrations of YO-NE (0.25, 0.5, 1, 3, 5 mg/mL) were found to have $96.62 \pm 1.44\%$, $83.29 \pm 2.52\%$, $82.30 \pm 2.64\%$, $81.69 \pm 1.24\%$, $67.95 \pm 0.80\%$ cell viability in HaCaT cells, respectively ($p < 0.05$). However, the concentrations of YO-NE tested (except 5 mg/mL: low cytotoxicity) did not show any cytotoxic effect on HaCaT cells. As shown in Figure 6, concentrations of 0.25 mg/mL, 0.5 mg/mL, 1 mg/mL, and 3 mg/mL YO-NE formulation had over 80% cell viability compared to the control group. This result indicates that the encapsulation of YO with NE makes it more cytocompatible compared to YO. Similar results were reported in literature (70,77,78).

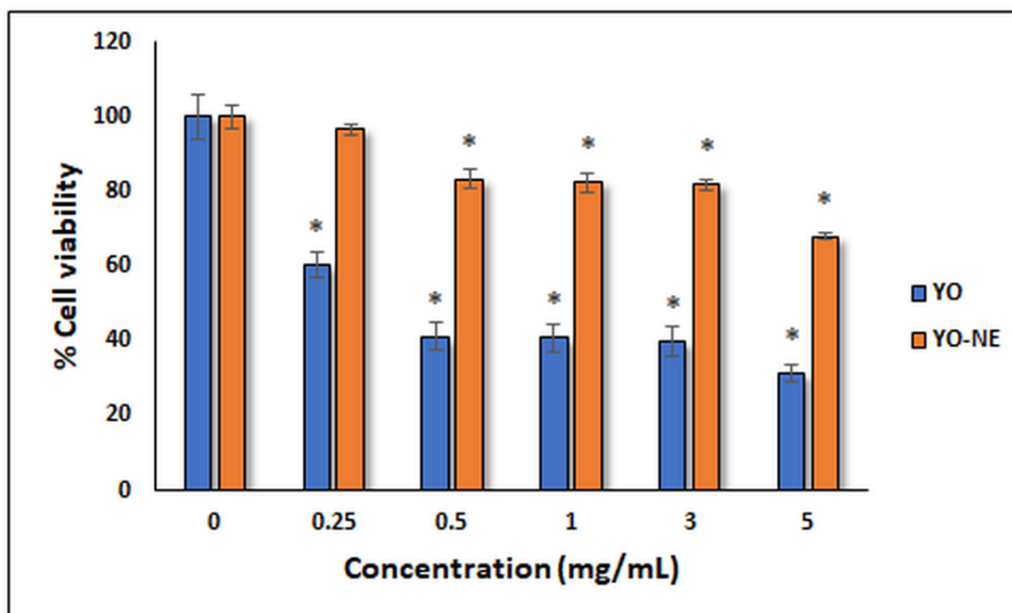


Figure 6: Cytotoxicity data of YO and YO-NE on HaCaT cells. The asterisk (*) indicates that the difference between the control group and the treatment groups is significant at the $p < 0.05$ level.

Solubility, instability and toxicity of lipophilic drugs pose problems. One of the most effective solutions to target these drugs is the formulation of NEs of lipophilic nutraceuticals. The solubility of lipophilic compounds increases as they disperse in the aqueous phase of the emulsion, preventing them from coming into direct contact with body fluids and tissues, thus reducing toxicity. Moreover, NEs provide high bioavailability of small amounts of encapsulated lipophilic substance to cells. They can, therefore, be used to study the uptake of encapsulated drug-active substance in cell cultures, improve the growth conditions and viability of cells, and conduct *in vitro* toxicity studies of lipophilic drugs (79). MTT results showed lower cytotoxicity of YO-NE compared to YO, indicating the nanoemulsion's controlled release properties and that YO's encapsulation is a suitable strategy to reduce its cytotoxicity towards HaCaT cells. Compared to YO, YO-NE still showed high biocompatibility even at higher concentrations and did not significantly affect HaCaT cell viability (80).

3.9. Analysis of Physicochemical and Pharmacokinetic Properties of Linalool and Germacrene-D

Kalagatur et al. (2018) (11) characterized ylang-ylang oil by GC-MS and reported that the main compounds in the oil's structure were linalool (29.15%), germacrene-D (11.82%), and thymol (8.45%). Physicochemical and pharmacokinetic analyses were performed to determine whether linalool and germacrene-D compounds in ylang-ylang oil are drugs (33). Various molecular properties such as absorption, distribution, metabolism, excretion, and structural properties such as molecular weight, number of hydrogen bond acceptors or donors, lipophilicity, and molar refractivity were investigated (39).

The physicochemical and pharmacokinetic properties of the compounds (Linalool, Germacrene-D) are

shown in Table 4 and Table 5. The Bioavailability Radar was displayed when predicting physicochemical properties such as lipophilicity, size, polarity, solubility, flexibility, and saturation (Figure 7). The radar plot shows that the selected compounds linalool and germacrene-D are within the pink area. This indicates a good bioavailability profile for the compounds and better drug similarity of the compounds alone. The pink area, the radar plot of molecules following Lipinski's rule of five, means that it is drug-like. According to Lipinski's rule of five, in order for a chemical compound to be orally active in humans, it must fulfill at least three of the following criteria: molecular weight ≤ 500 , XLOGP3 < 3.5 , hydrogen bond acceptor ≤ 10 , hydrogen bond donor ≤ 5 and molar refractivity = 40-130 (36). In our study, Linalool complies with the rule of five. Germacrene-D violated the rule of one since MLOGP > 4.15 . These two chemical compounds were accepted as drug analogs as drug as they met the Lipinski's rules. Therefore, ylang-ylang oil containing these chemical compounds has a high potential to be drug analogs (55).

The bioavailability of a drug depends on the absorption processes and first-pass metabolism in the liver, which depends on the solubility and permeability of the compound. Drugs with optimum log P and low molecular mass (< 500) also have high permeability (81). In our study, these two compounds have high Caco-2 cell permeability as the permeability (nm/sec) > 0.90 . The selected linalool and germacrene-D compounds exhibited negative Log Kp values (skin permeability) of -1.737 and -1.429, indicating that they may be suitable as promising compounds for transdermal delivery.

James et al. (2023) (82) found the log Kp value of the linalool compound to be -1.43. Drioiche et al. (2023) (83) found the log Kp value of Germacrene-D compound to be -1.429. In estimating skin permeability, the log Kp value should be in the range

of -8.0 to -1.0. In this study, the Log Kp values of linalool and germacrene-D compounds were found in the recommended range and similar to the studies in

the literature. These results ensure good dermal penetration of these compounds.

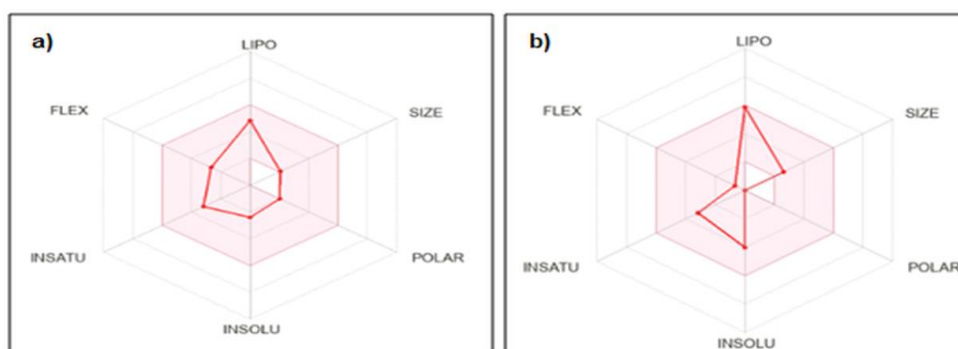


Figure 7: Bioavailability radar showing and signaling drug susceptibility to Linalool (a) and Germacrene-D (b)

CYP450 and its isoforms belong to the hemoprotein family and play an important role in drug metabolism and clearance. Inhibition of isoforms leads to lower clearance and accumulation of the drug or its metabolism. Gastrointestinal (GI) absorption indicates the capacity of the drug to be absorbed and pass into the bloodstream. A compound without CYP450 inhibition and with high GI absorption properties implies that the compound has a good capacity for metabolization and absorption (39). In our study, Linalool and Germacrene-D compounds did not cause CYP450 inhibition and showed high GI

absorption of over 90%. The ability of a drug to cross the blood-brain barrier and enter the brain is a parameter that must be taken into account to help reduce or ameliorate side effects and toxicity (37). These two compounds provided values above $\log BB > 0.3$ and were found to be easily and well distributed into the brain and thus, able to bind to specific receptors. These two compounds showed good drug clearance values, and neither was a substrate for organic cation transporter 2 (OCT2). Furthermore, no hERG 1 channel inhibition or toxicity was predicted from the compounds.

Table 4: Linalool and Germacrene-D ADMET Properties.

Property	Physicochemical properties	Linalool	Germacrene-D
Absorption	Water solubility (log mol/L)	-2.612	-5.682
	Caco-2 permeability (log Papp in 10^{-6} cm/s)	1.493	1.436
	Intestinal absorption (human) (% Absorbed)	93.163	95.59
	Skin Permeability (log Kp)	-1.737	-1.429
	P-glycoprotein substrate (Yes/No)	No	No
	P-glycoprotein I inhibitor (Yes/No)	No	No
	P-glycoprotein II inhibitor (Yes/No)	No	No
Distribution	VDss (human) (log L/kg)	0.152	0.544
	Fraction unbound (human) (Fu)	0.484	0.261
	BBB permeability (log BB)	0.598	0.723
	CNS permeability (log PS)	-2.339	-2.138
Metabolism	CYP2D6 substrate (Yes/No)	No	No
	CYP3A4 substrate (Yes/No)	No	No
	CYP1A2 inhibitor (Yes/No)	No	No
	CYP2C19 inhibitor (Yes/No)	No	No
	CYP2C9 inhibitor (Yes/No)	No	No
	CYP2D6 inhibitor (Yes/No)	No	No
	CYP3A4 inhibitor (Yes/No)	No	No
Excretion	Total Clearance (log ml/min/kg)	0.446	1.42
	Renal OCT2 substrate (Yes/No)	No	No
Toxicity	AMES toxicity (Yes/No)	No	No
	Max. tolerated dose (human) (log mg/kg/day)	0.774	0.497
	hERG I inhibitor (Yes/No)	No	No
	hERG II inhibitor (Yes/No)	No	No
	Oral Rat Acute Toxicity (LD50)	1.704	1.634
	Oral Rat Chronic Toxicity (LOAEL)	2.024	1.413
	Hepatotoxicity (Yes/No)	No	No
	Skin Sensitisation (Yes/No)	Yes	Yes
	<i>T. pyriformis</i> toxicity (log ug/L)	0.515	1.671
	Minnow toxicity (log mM)	1.277	0.257

Table 5: Physicochemical properties of Linalool and Germacrene-D.

Physicochemical properties	Linalool	Germacrene-D
Formula	C ₁₀ H ₁₈ O	C ₁₅ H ₂₄
Molecular weight	154.25 g/mol	204.357 g/mol
Number of heavy atoms	11	15
Number of aromatic heavy atoms	0	0
Fraction Csp ³	0.60	0.60
Number of rotatable bonds	4	1
Number of H-bond acceptors	1	0
Number of H-bond donors	1	0
Log P	2.6698	4.8913
Molar Refractivity	50.44	70.68
TPSA	20.23 Å ²	0.00 Å ²
Lipophilicity		
Log Po/w (XLOGP3)	2.97	4.74
Water solubility		
Log S (ESOL)	-2.40 6.09x10 ⁻¹ mg/mL; 3.95x10 ⁻³ mol/L Soluble	-4.03 1.92x10 ⁻² mg/mL; 9.39x10 ⁻⁵ mol/L Moderately soluble

3.10. Biological Activity Analysis of Linalool and Germacrene-D

The biological activity properties of Linalool and Germacrene-D compounds are presented in Table 6. Possible biological activities of Linalool and Germacrene-D compounds were obtained by the PASS server. Additionally, the set of pharmacological effects, mechanisms of action, and specific toxicities that may be exhibited by a compound in its interaction with biological entities were predicted by the PASS server (84). The software estimates the

predicted activity spectrum of a compound into probable activity (Pa) and probable inactivity (Pi). Only activities where Pa > Pi are considered possible for a given compound. If Pa > 0.7, the probability of experimental pharmacological effect is high, if 0.5 < Pa < 0.7, the probability of experimental pharmacological effect is less, when Pa < 0.5, the chance of finding the activity experimentally is less, but it may indicate the chance of finding a new compound (40).

Table 6: Biological activities of Linalool and Germacrene.

Components	Pa	Pi	Activity
Linalool	0.978	0.002	Mucomembranous protector
	0.913	0.003	Cell adhesion molecule inhibitor
	0.896	0.009	Aspulvinone dimethylallyltransferase inhibitor
	0.868	0.003	Fatty-acyl-CoA synthase inhibitor
	0.860	0.007	Beta-adrenergic receptor kinase inhibitor
	0.860	0.007	G-protein-coupled receptor kinase inhibitor
	0.836	0.002	Ecdysone 20-monooxygenase inhibitor
	0.832	0.002	BRAF expression inhibitor
	0.803	0.005	Lipid metabolism regulator
	0.798	0.004	Antisecretoric
	0.808	0.017	Antieczematic
	0.781	0.004	Undecaprenyl-phosphate mannosyltransferase inhibitor
	0.711	0.002	Antiviral (Rhinovirus)
0.719	0.022	TP53 expression enhancer	
Germacrene-D	0.915	0.004	Antieczematic
	0.885	0.002	Carminative
	0.817	0.010	Antineoplastic
	0.732	0.002	Testosterone agonist
	0.712	0.011	Phosphatase inhibitor
	0.714	0.064	Ubiquinol-cytochrome-c reductase inhibitor

Linalool contributes to topical anti-inflammatory and analgesic activities by inhibiting COX-2 protein expression in inflammatory tissues and reducing oxidative stress (85). Germacrene D reduces inflammation by preventing the release of inflammatory mediators by inactivating the enzymes that cause inflammation. One of the main mechanisms of Germacrene D is the inhibition of

prostaglandin synthesis. Prostaglandins are compounds that affect the inflammatory response and pain generation. This inhibition both alleviates inflammation and reduces pain generation (86). Linalool and Germacrene-D compounds play an essential role in the pathogenesis of inflammatory diseases. These compounds inhibit cell adhesion molecules involved in leukocyte traffic to provide

therapeutic intervention for leukocytes. With these properties, it is known to have therapeutic potential in human inflammatory disorders (87). These compounds exhibit various biological activities such as mucomembranous protector, cell adhesion molecule inhibitor, antisecretory, and antieczematic. It is understood that these compounds may be involved in the regulation of dermatological diseases caused by inflammation, with their remarkable anti-inflammatory activities, as they have high pharmacological activity values ($Pa > 0.7$).

4. CONCLUSION

UV rays can cause various damage to the skin, such as erythema, pigment change, photoaging and skin cancer. Essential oils can contribute to the prevention or treatment of damage to the skin caused by UV rays due to their UV protective properties. In our study, YO essential oil was used to protect against UV damage with its anti-inflammatory and antioxidant properties. YO was formulated in the NE dosage form to provide features such as increased skin permeability, bioavailability, solubility, therapeutic activity, stability, and controlled release. YO-NE was obtained with suitable average droplet size, PdI, and the ζ potential values, highly thermodynamically stable without sedimentation or phase separation, pH, and conductivity values suitable for topical application. It was determined that almost all the YO in the NE formulation was released within five hours. Cytotoxicity results showed that NE reduced the cytotoxicity of YO, and the YO-NE formulation had no toxicity. In conclusion, YO could be a formulation candidate that can be applied topically in treating dermatological diseases due to its controlled release feature, formulated in NE dosage form, non-toxicity, and the unique biological activities of Linalool and Germacrene-D compounds.

5. CONFLICT OF INTEREST

No conflict of interest.

6. ACKNOWLEDGMENTS

This work was supported by Yildiz Technical University Scientific Research Foundation [FCD-2021-4509]. In this study, the infrastructure of the Applied Nanotechnology and Antibody Production Laboratory established with TUBITAK support (project numbers: 115S132, 117S097 and 5200110) was used. The authors would also like to thank TUBITAK for their support.

7. REFERENCES

1. Kammeyer A, Luiten RM. Oxidation events and skin aging. *Ageing Res Rev* [Internet]. 2015 May;21:16–29. Available from: [<URL>](#).
2. Nanni V, Canuti L, Gismondi A, Canini A. Hydroalcoholic extract of *Spartium junceum* L. flowers inhibits growth and melanogenesis in B16-F10 cells by inducing senescence. *Phytomedicine*

[Internet]. 2018 Jul;46:1–10. Available from: [<URL>](#).

3. Rabe JH, Mamelak AJ, McElgunn PJS, Morison WL, Sauder DN. Photoaging: Mechanisms and repair. *J Am Acad Dermatol* [Internet]. 2006 Jul;55(1):1–19. Available from: [<URL>](#).

4. Zhu S, Zhao Z, Qin W, Liu T, Yang Y, Wang Z, et al. The Nanostructured lipid carrier gel of Oroxylin A reduced UV-induced skin oxidative stress damage. *Colloids Surfaces B Biointerfaces* [Internet]. 2022 Aug;216:112578. Available from: [<URL>](#).

5. González S, Fernández-Lorente M, Gilaberte-Calzada Y. The latest on skin photoprotection. *Clin Dermatol* [Internet]. 2008 Nov;26(6):614–26. Available from: [<URL>](#).

6. Mukherjee S, Date A, Patravale V, Korting HC, Roeder A, Weindl G. Retinoids in the treatment of skin aging: an overview of clinical efficacy and safety. *Clin Interv Aging* [Internet]. 2006 Dec;1(4):327–48. Available from: [<URL>](#).

7. Pacheco MT, Silva ACG, Nascimento TL, Diniz DGA, Valadares MC, Lima EM. Protective effect of sucupira oil nanoemulsion against oxidative stress in UVA-irradiated HaCaT cells. *J Pharm Pharmacol* [Internet]. 2019 Sep 3;71(10):1532–43. Available from: [<URL>](#).

8. Guzmán E, Lucia A. Essential Oils and Their Individual Components in Cosmetic Products. *Cosmetics* [Internet]. 2021 Dec 3;8(4):114. Available from: [<URL>](#).

9. Sedky NK, Abdel-Kader NM, Issa MY, Abdelhady MMM, Shamma SN, Bakowsky U, et al. Co-Delivery of Ylang Ylang Oil of *Cananga odorata* and Oxaliplatin Using Intelligent pH-Sensitive Lipid-Based Nanovesicles for the Effective Treatment of Triple-Negative Breast Cancer. *Int J Mol Sci* [Internet]. 2023 May 7;24(9):8392. Available from: [<URL>](#).

10. Goodrich KR. Floral scent in Annonaceae. *Bot J Linn Soc* [Internet]. 2012 May;169(1):262–79. Available from: [<URL>](#).

11. Kalagatur NK, Mudili V, Kamasani JR, Siddaiah C. Discrete and combined effects of Ylang-Ylang (*Cananga odorata*) essential oil and gamma irradiation on growth and mycotoxins production by *Fusarium graminearum* in maize. *Food Control* [Internet]. 2018 Dec;94:276–83. Available from: [<URL>](#).

12. Upadhyay N, Singh VK, Dwivedy AK, Chaudhari AK, Dubey NK. Assessment of nanoencapsulated *Cananga odorata* essential oil in chitosan nanopolymer as a green approach to boost the antifungal, antioxidant and in situ efficacy. *Int J Biol Macromol* [Internet]. 2021 Feb;171:480–90. Available from: [<URL>](#).

13. Youness RA, Al-Mahallawi AM, Mahmoud FH, Atta H, Braoudaki M, Fahmy SA. Oral Delivery of Psoralidin by Mucoadhesive Surface-Modified Bilosomes Showed Boosted Apoptotic and Necrotic

- Effects against Breast and Lung Cancer Cells. *Polymers (Basel)* [Internet]. 2023 Mar 15;15(6):1464. Available from: [<URL>](#).
14. Fahmy SA, Ponte F, Fawzy IM, Sicilia E, Azzazy HMES. Betaine host-guest complexation with a calixarene receptor: enhanced in vitro anticancer effect. *RSC Adv* [Internet]. 2021;11(40):24673–80. Available from: [<URL>](#).
15. Azzazy HMES, Sawy AM, Abdelnaser A, Meselhy MR, Shoeib T, Fahmy SA. Peganum harmala Alkaloids and Tannic Acid Encapsulated in PAMAM Dendrimers: Improved Anticancer Activities as Compared to Doxorubicin. *ACS Appl Polym Mater* [Internet]. 2022 Oct 14;4(10):7228–39. Available from: [<URL>](#).
16. Fahmy SA, Mahdy NK, Al Mulla H, ElMeshad AN, Issa MY, Azzazy HMES. PLGA/PEG Nanoparticles Loaded with Cyclodextrin-Peganum harmala Alkaloid Complex and Ascorbic Acid with Promising Antimicrobial Activities. *Pharmaceutics* [Internet]. 2022 Jan 7;14(1):142. Available from: [<URL>](#).
17. Kong M, Park HJ. Stability investigation of hyaluronic acid based nanoemulsion and its potential as transdermal carrier. *Carbohydr Polym* [Internet]. 2011 Jan 30;83(3):1303–10. Available from: [<URL>](#).
18. Soriano-Ruiz JL, Calpena-Capmany AC, Cañadas-Enrich C, Febrer NB de, Suñer-Carbó J, Souto EB, et al. Biopharmaceutical profile of a clotrimazole nanoemulsion: Evaluation on skin and mucosae as anticandidal agent. *Int J Pharm* [Internet]. 2019 Jan;554:105–15. Available from: [<URL>](#).
19. Thomas L, Zakir F, Mirza MA, Anwer MK, Ahmad FJ, Iqbal Z. Development of Curcumin loaded chitosan polymer based nanoemulsion gel: In vitro, ex vivo evaluation and in vivo wound healing studies. *Int J Biol Macromol* [Internet]. 2017 Aug;101:569–79. Available from: [<URL>](#).
20. Echeverría J, Albuquerque R. Nanoemulsions of Essential Oils: New Tool for Control of Vector-Borne Diseases and In Vitro Effects on Some Parasitic Agents. *Medicines* [Internet]. 2019 Mar 27;6(2):42. Available from: [<URL>](#).
21. Jaiswal M, Dudhe R, Sharma PK. Nanoemulsion: an advanced mode of drug delivery system. *3 Biotech* [Internet]. 2015 Apr 8;5(2):123–7. Available from: [<URL>](#).
22. Sharadha M, Gowda D V, Vishal Gupta N, Akhila AR. An overview on topical drug delivery system—updated review. *Int J Res Pharm Sci* [Internet]. 2020;11(1):368–85. Available from: [<URL>](#).
23. Ghosh V, Saranya S, Mukherjee A, Chandrasekaran N. Cinnamon Oil Nanoemulsion Formulation by Ultrasonic Emulsification: Investigation of Its Bactericidal Activity. *J Nanosci Nanotechnol* [Internet]. 2013 Jan 1;13(1):114–22. Available from: [<URL>](#).
24. Gul U, Khan MI, Madni A, Sohail MF, Rehman M, Rasul A, et al. Olive oil and clove oil-based nanoemulsion for topical delivery of terbinafine hydrochloride: in vitro and ex vivo evaluation. *Drug Deliv* [Internet]. 2022 Dec 31;29(1):600–12. Available from: [<URL>](#).
25. Ozkan B, Altuntas E, Cakir Koc R, Budama-Kilinc Y. Development of piperine nanoemulsions: an alternative topical application for hypopigmentation. *Drug Dev Ind Pharm* [Internet]. 2022 Mar 4;48(3):117–27. Available from: [<URL>](#).
26. Budama-Kilinc Y, Gok B, Kecel-Gunduz S, Altuntas E. Development of nanoformulation for hyperpigmentation disorders: Experimental evaluations, in vitro efficacy and in silico molecular docking studies. *Arab J Chem* [Internet]. 2022 Dec;15(12):104362. Available from: [<URL>](#).
27. Gaba B, Khan T, Haider MF, Alam T, Baboota S, Parvez S, et al. Vitamin E Loaded Naringenin Nanoemulsion via Intranasal Delivery for the Management of Oxidative Stress in a 6-OHDA Parkinson's Disease Model. *Biomed Res Int* [Internet]. 2019 Apr 14;2019:2382563. Available from: [<URL>](#).
28. Ercin E, Kecel-Gunduz S, Gok B, Aydin T, Budama-Kilinc Y, Kartal M. Laurus nobilis L. Essential Oil-Loaded PLGA as a Nanoformulation Candidate for Cancer Treatment. *Molecules* [Internet]. 2022 Mar 15;27(6):1899. Available from: [<URL>](#).
29. Rashid SA, Bashir S, Naseem F, Farid A, Rather IA, Hakeem KR. Olive Oil Based Methotrexate Loaded Topical Nanoemulsion Gel for the Treatment of Imiquimod Induced Psoriasis-like Skin Inflammation in an Animal Model. *Biology (Basel)* [Internet]. 2021 Oct 31;10(11):1121. Available from: [<URL>](#).
30. Budama-Kilinc Y, Kecel-Gunduz S, Ozdemir B, Bicak B, Akman G, Arvas B, et al. New nanodrug design for cancer therapy: Its synthesis, formulation, in vitro and in silico evaluations. *Arch Pharm (Weinheim)* [Internet]. 2020 Nov 5;353(11):2000137. Available from: [<URL>](#).
31. Gok B, Budama-Kilinc Y, Kecel-Gunduz S. Anti-aging activity of Syn-Ake peptide by in silico approaches and in vitro tests. *J Biomol Struct Dyn* [Internet]. 2024 Jul 2;42(10):5015–29. Available from: [<URL>](#).
32. Gunaseelan S, Balupillai A, Govindasamy K, Ramasamy K, Muthusamy G, Shanmugam M, et al. Linalool prevents oxidative stress activated protein kinases in single UVB-exposed human skin cells. Slominski AT, editor. *PLoS One* [Internet]. 2017 May 3;12(5):e0176699. Available from: [<URL>](#).
33. Haque MI, Khalipha ABR, Sakib MR, Prottay AAS, Islam MA, Zannat R, et al. In-Silico Molecular Docking Study of Linalool Against 3ELJ for Cell Cycle Arrest and Apoptosis in HEPG2 Cells. *Int J Evergr Sci Res* [Internet]. 2021;3(2):105–18. Available from: [<URL>](#).
34. Steliopoulos P, Wüst M, Adam KP, Mosandl A. Biosynthesis of the sesquiterpene germacrene D in *Solidago canadensis*: 13C and 2H labeling studies.

- Phytochemistry [Internet]. 2002 May;60(1):13–20. Available from: [<URL>](#).
35. Prosser I, Altug IG, Phillips AL, König WA, Bouwmeester HJ, Beale MH. Enantiospecific (+)- and (-)-germacrene D synthases, cloned from goldenrod, reveal a functionally active variant of the universal isoprenoid-biosynthesis aspartate-rich motif. *Arch Biochem Biophys* [Internet]. 2004 Dec;432(2):136–44. Available from: [<URL>](#).
36. Daina A, Michielin O, Zoete V. SwissADME: a free web tool to evaluate pharmacokinetics, drug-likeness and medicinal chemistry friendliness of small molecules. *Sci Rep* [Internet]. 2017 Mar 3;7(1):42717. Available from: [<URL>](#).
37. Pires DE V, Blundell TL, Ascher DB. pkCSM: Predicting Small-Molecule Pharmacokinetic and Toxicity Properties Using Graph-Based Signatures. *J Med Chem* [Internet]. 2015 May 14;58(9):4066–72. Available from: [<URL>](#).
38. Lipinski CA, Lombardo F, Dominy BW, Feeney PJ. Experimental and computational approaches to estimate solubility and permeability in drug discovery and development settings. *Adv Drug Deliv Rev* [Internet]. 2001 Mar;46(1–3):3–26. Available from: [<URL>](#).
39. Rakhecha B, Agnihotri P, Dakal TC, Saquib M, Monu, Biswas S. Anti-inflammatory activity of nicotine isolated from *Brassica oleracea* in rheumatoid arthritis. *Biosci Rep* [Internet]. 2022 Apr 29;42(4):BSR20211392. Available from: [<URL>](#).
40. Mojumdar M, Kabir MSH, Hasan MS, Ahmed T, Rahman MR, Akter Y, et al. Molecular docking and pass prediction for analgesic activity of some isolated compounds from *Acalypha indica* L. and ADME/T property analysis of the compounds. *World J Pharm Res* [Internet]. 2016;5(7):1761–70. Available from: [<URL>](#).
41. Zhao D, Ge Y, Xiang X, Dong H, Qin W, Zhang Q. Structure and stability characterization of pea protein isolate-xylan conjugate-stabilized nanoemulsions prepared using ultrasound homogenization. *Ultrason Sonochem* [Internet]. 2022 Nov;90:106195. Available from: [<URL>](#).
42. Manzoor M, Sharma P, Murtaza M, Jaiswal AK, Jaglan S. Fabrication, characterization, and interventions of protein, polysaccharide and lipid-based nanoemulsions in food and nutraceutical delivery applications: A review. *Int J Biol Macromol* [Internet]. 2023 Jun;241:124485. Available from: [<URL>](#).
43. Kapoor A, Preet S. Evaluation of Acaricidal Activity of Cinnamomum camphora (F. Lauraceae) Essential Oil Nanoemulsion Against Cattle Tick *Rhipicephalus microplus*. *Adv Zool Bot* [Internet]. 2023 Apr;11(2):121–8. Available from: [<URL>](#).
44. Rupa E, Li J, Arif M, Yaxi H, Puja A, Chan A, et al. *Cordyceps militaris* Fungus Extracts-Mediated Nanoemulsion for Improvement Antioxidant, Antimicrobial, and Anti-Inflammatory Activities. *Molecules* [Internet]. 2020 Dec 4;25(23):5733. Available from: [<URL>](#).
45. Ayllón-Gutiérrez R, López-Maldonado EA, Macías-Alonso M, González Marrero J, Díaz-Rubio L, Córdova-Guerrero I. Evaluation of the Stability of a 1,8-Cineole Nanoemulsion and Its Fumigant Toxicity Effect against the Pests *Tetranychus urticae*, *Rhopalosiphum maidis* and *Bemisia tabaci*. *Insects* [Internet]. 2023 Jul 24;14(7):663. Available from: [<URL>](#).
46. Liu Q, Huang H, Chen H, Lin J, Wang Q. Food-Grade Nanoemulsions: Preparation, Stability and Application in Encapsulation of Bioactive Compounds. *Molecules* [Internet]. 2019 Nov 21;24(23):4242. Available from: [<URL>](#).
47. Gorjian H, Mihankhah P, Khaligh NG. Influence of tween nature and type on physicochemical properties and stability of spearmint essential oil (*Mentha spicata* L.) stabilized with basil seed mucilage nanoemulsion. *J Mol Liq* [Internet]. 2022 Aug;359:119379. Available from: [<URL>](#).
48. Mohammed NK, Muhiaddin BJ, Meor Hussin AS. Characterization of nanoemulsion of *Nigella sativa* oil and its application in ice cream. *Food Sci Nutr* [Internet]. 2020 Jun 21;8(6):2608–18. Available from: [<URL>](#).
49. Kampa J, Frazier R, Rodriguez-Garcia J. Physical and Chemical Characterisation of Conventional and Nano/Emulsions: Influence of Vegetable Oils from Different Origins. *Foods* [Internet]. 2022 Feb 25;11(5):681. Available from: [<URL>](#).
50. Lima TS, Silva MFS, Nunes XP, Colombo A V, Oliveira HP, Goto PL, et al. Cineole-containing nanoemulsion: Development, stability, and antibacterial activity. *Chem Phys Lipids* [Internet]. 2021 Sep;239:105113. Available from: [<URL>](#).
51. Özdemir S, Üner B, Karaküçük A, Çelik B, Sümer E, Taş Ç. Nanoemulsions as a Promising Carrier for Topical Delivery of Etodolac: Formulation Development and Characterization. *Pharmaceutics* [Internet]. 2023 Oct 23;15(10):2510. Available from: [<URL>](#).
52. Gündel S da S, de Godoi SN, Santos RCV, da Silva JT, Leite LB de M, Amaral AC, et al. In vivo antifungal activity of nanoemulsions containing eucalyptus or lemongrass essential oils in murine model of vulvovaginal candidiasis. *J Drug Deliv Sci Technol* [Internet]. 2020 Jun;57:101762. Available from: [<URL>](#).
53. Lunardi CN, Gomes AJ, Rocha FS, De Tommaso J, Patience GS. Experimental methods in chemical engineering: Zeta potential. *Can J Chem Eng* [Internet]. 2021 Mar 12;99(3):627–39. Available from: [<URL>](#).
54. Dheyab MA, Aziz AA, Jameel MS, Noqta OA, Khaniabadi PM, Mehrdel B. Simple rapid stabilization method through citric acid modification for magnetite nanoparticles. *Sci Rep* [Internet]. 2020 Jul 1;10(1):10793. Available from: [<URL>](#).

55. Kildaci I, Budama-Kilinc Y, Kecel-Gunduz S, Altuntas E. Linseed Oil Nanoemulsions for treatment of Atopic Dermatitis disease: Formulation, characterization, in vitro and in silico evaluations. *J Drug Deliv Sci Technol* [Internet]. 2021 Aug;64:102652. Available from: [<URL>](#).
56. Gok B, Budama Kilinc Y. Chlorogenic acid nanoemulsion for staphylococcus aureus causing skin infection: Synthesis, characterization and evaluation of antibacterial efficacy. *Sigma J Eng Nat Sci* [Internet]. 2022 Aug;41(2):322–30. Available from: [<URL>](#).
57. Marhamati M, Ranjbar G, Rezaie M. Effects of emulsifiers on the physicochemical stability of Oil-in-water Nanoemulsions: A critical review. *J Mol Liq* [Internet]. 2021 Oct;340:117218. Available from: [<URL>](#).
58. Rashid SA, Bashir S, Ullah H, Khan DH, Shah PA, Danish MZ, et al. Development, characterization and optimization of methotrexate-olive oil nano-emulsion for topical application. *Pak J Pharm Sci* [Internet]. 2021;34. Available from: [<URL>](#).
59. Hammadi ID, N. Abd Alhammid S. Preparation and Characterization of Topical Letrozole Nanoemulsion for Breast Cancer. *Iraqi J Pharm Sci* [Internet]. 2020 Jun 25;29(1):195–206. Available from: [<URL>](#).
60. Roselan MA, Ashari SE, Faujan NH, Mohd Faudzi SM, Mohamad R. An Improved Nanoemulsion Formulation Containing Kojic Monooleate: Optimization, Characterization and In Vitro Studies. *Molecules* [Internet]. 2020 Jun 4;25(11):2616. Available from: [<URL>](#).
61. Wang L, Guan X, Zheng C, Wang N, Lu H, Huang Z. New Low-Energy Method for Nanoemulsion Formation: pH Regulation Based on Fatty Acid/Amine Complexes. *Langmuir* [Internet]. 2020 Sep 1;36(34):10082–90. Available from: [<URL>](#).
62. Altuntaş E, Yener G. Formulation and Evaluation of Thermoreversible In Situ Nasal Gels Containing Mometasone Furoate for Allergic Rhinitis. *AAPS PharmSciTech* [Internet]. 2017 Oct 9;18(7):2673–82. Available from: [<URL>](#).
63. Mat Hadzir N, Basri M, Abdul Rahman MB, Salleh AB, Raja Abdul Rahman RNZ, Basri H. Phase Behaviour and Formation of Fatty Acid Esters Nanoemulsions Containing Piroxicam. *AAPS PharmSciTech* [Internet]. 2013 Mar 6;14(1):456–63. Available from: [<URL>](#).
64. Guttoff M, Saberi AH, McClements DJ. Formation of vitamin D nanoemulsion-based delivery systems by spontaneous emulsification: Factors affecting particle size and stability. *Food Chem* [Internet]. 2015 Mar;171:117–22. Available from: [<URL>](#).
65. Bernardi DS, Pereira TA, Maciel NR, Bortoloto J, Viera GS, Oliveira GC, et al. Formation and stability of oil-in-water nanoemulsions containing rice bran oil: in vitro and in vivo assessments. *J Nanobiotechnology* [Internet]. 2011;9(1):44. Available from: [<URL>](#).
66. Altuntaş E, Yener G. Anti-aging potential of a cream containing herbal oils and honey: Formulation and in vivo evaluation of effectiveness using non-invasive biophysical techniques. *IOSR J Pharm Biol Sci* [Internet]. 2015;10(6):51–60. Available from: [<URL>](#).
67. Shen Y, Ni ZJ, Thakur K, Zhang JG, Hu F, Wei ZJ. Preparation and characterization of clove essential oil loaded nanoemulsion and pickering emulsion activated pullulan-gelatin based edible film. *Int J Biol Macromol* [Internet]. 2021 Jun;181:528–39. Available from: [<URL>](#).
68. Jerobin J, Sureshkumar RS, Anjali CH, Mukherjee A, Chandrasekaran N. Biodegradable polymer based encapsulation of neem oil nanoemulsion for controlled release of Aza-A. *Carbohydr Polym* [Internet]. 2012 Nov;90(4):1750–6. Available from: [<URL>](#).
69. Fopase R, Pathode SR, Sharma S, Datta P, Pandey LM. Lipopeptide and essential oil based nanoemulsion for controlled drug delivery. *Polym Technol Mater* [Internet]. 2020 Dec 11;59(18):2076–86. Available from: [<URL>](#).
70. Rajitha P, Shammika P, Aiswarya S, Gopikrishnan A, Jayakumar R, Sabitha M. Chaulmoogra oil based methotrexate loaded topical nanoemulsion for the treatment of psoriasis. *J Drug Deliv Sci Technol* [Internet]. 2019 Feb;49:463–76. Available from: [<URL>](#).
71. Mohd Narawi M, Chiu HI, Yong YK, Mohamad Zain NN, Ramachandran MR, Tham CL, et al. Biocompatible Nutmeg Oil-Loaded Nanoemulsion as Phyto-Repellent. *Front Pharmacol* [Internet]. 2020 Mar 17;11:214. Available from: [<URL>](#).
72. Shah J, Nair AB, Jacob S, Patel RK, Shah H, Shehata TM, et al. Nanoemulsion Based Vehicle for Effective Ocular Delivery of Moxifloxacin Using Experimental Design and Pharmacokinetic Study in Rabbits. *Pharmaceutics* [Internet]. 2019 May 11;11(5):230. Available from: [<URL>](#).
73. Botros SR, Hussein AK, Mansour HF. A Novel Nanoemulsion Intermediate Gel as a Promising Approach for Delivery of Itraconazole: Design, In Vitro and Ex Vivo Appraisal. *AAPS PharmSciTech* [Internet]. 2020 Oct 6;21(7):272. Available from: [<URL>](#).
74. Roggia I, Gomes P, Dalcin AJF, Ourique AF, Mânica da Cruz IB, Ribeiro EE, et al. Profiling and Evaluation of the Effect of Guarana-Loaded Liposomes on Different Skin Cell Lines: An In Vitro Study. *Cosmetics* [Internet]. 2023 May 12;10(3):79. Available from: [<URL>](#).
75. Serrano I, Alinho B, Cunha E, Tavares L, Trindade A, Oliveira M. Bacteriostatic and Antibiofilm Efficacy of a Nisin Z Solution against Co-Cultures of *Staphylococcus aureus* and *Pseudomonas aeruginosa*

- from Diabetic Foot Infections. *Life* [Internet]. 2023 Feb 11;13(2):504. Available from: [<URL>](#).
76. Standard I. Biological evaluation of medical devices—Part 5: Tests for in vitro cytotoxicity. Geneva, Switz Int Organ Stand. 2009;
77. Caldeira LR, Fernandes FR, Costa DF, Frézard F, Afonso LCC, Ferreira LAM. Nanoemulsions loaded with amphotericin B: A new approach for the treatment of leishmaniasis. *Eur J Pharm Sci* [Internet]. 2015 Apr;70:125–31. Available from: [<URL>](#).
78. Musa SH, Razali FN, Shamsudin N, Salim N, Basri M. Novel topical nano-colloidal carrier loaded with cyclosporine: Biological evaluation potentially for psoriasis treatment. *J Drug Deliv Sci Technol* [Internet]. 2021 Jun;63:102440. Available from: [<URL>](#).
79. Meghani N, Patel P, Kansara K, Ranjan S, Dasgupta N, Ramalingam C, et al. Formulation of vitamin D encapsulated cinnamon oil nanoemulsion: Its potential anti-cancerous activity in human alveolar carcinoma cells. *Colloids Surfaces B Biointerfaces* [Internet]. 2018 Jun;166:349–57. Available from: [<URL>](#).
80. Liao S, Yang G, Wang Z, Ou Y, Huang S, Li B, et al. Ultrasonic preparation of Tween-essential oil (*Zanthoxylum schinifolium* Sieb. et Zucc) oil/water nanoemulsion: Improved stability and alleviation of *Staphylococcus epidermidis* biofilm. *Ind Crops Prod* [Internet]. 2022 Nov;188:115654. Available from: [<URL>](#).
81. Singh I, Morris A. Performance of transdermal therapeutic systems: Effects of biological factors. *Int J Pharm Investig* [Internet]. 2011;1(1):4. Available from: [<URL>](#).
82. James JP, Ail PD, Crasta L, Kamath RS, Shura MH, T.J S. In Silico ADMET and Molecular Interaction Profiles of Phytochemicals from Medicinal Plants in Dakshina Kannada. *J Heal Allied Sci NU* [Internet]. 2024 Apr 19;14(2):190–201. Available from: [<URL>](#).
83. Drioiche A, Ailli A, Remok F, Saidi S, Gourich AA, Asbabou A, et al. Analysis of the Chemical Composition and Evaluation of the Antioxidant, Antimicrobial, Anticoagulant, and Antidiabetic Properties of *Pistacia lentiscus* from Boulemane as a Natural Nutraceutical Preservative. *Biomedicines* [Internet]. 2023 Aug 24;11(9):2372. Available from: [<URL>](#).
84. Jamuna S, Rathinavel A, Mohammed Sadullah S, Devaraj S. In silico approach to study the metabolism and biological activities of oligomeric proanthocyanidin complexes. *Indian J Pharmacol* [Internet]. 2018;50(5):242–50. Available from: [<URL>](#).
85. Li XJ, Yang YJ, Li YS, Zhang WK, Tang HB. α -Pinene, linalool, and 1-octanol contribute to the topical anti-inflammatory and analgesic activities of frankincense by inhibiting COX-2. *J Ethnopharmacol* [Internet]. 2016 Feb;179:22–6. Available from: [<URL>](#).
86. Amanpour A, Çelebi F, Kahraman IG, Çelik F. Diyet İnflamatuvar İndeksi, İnflamasyon ve Beslenme. *Türkiye Sağlık Bilim ve Araştırmaları Derg* [Internet]. 2022 Dec 29;5(3):59–80. Available from: [<URL>](#).
87. Ulbrich H, Eriksson EE, Lindbom L. Leukocyte and endothelial cell adhesion molecules as targets for therapeutic interventions in inflammatory disease. *Trends Pharmacol Sci* [Internet]. 2003 Dec;24(12):640–7. Available from: [<URL>](#).

